Non-explosive methods for simulating blast loading of structures with complex geometries

Peter Huson, Robert J. Asaro*, Lauren Stewart, Gilbert A. Hegemier

Department of Structural Engineering, University of California, San Diego, La Jolla, CA 92093, USA

A B S T R A C T

Characterizing structural responses and applied loads during the entire course of a blast event is problematic due to the harsh conditions of the explosive environment. A procedure for the distribution of blast-like pressures to structures of complex geometries using custom water bladders has been developed using the University of California, San Diego's (UCSD) Blast Simulator. The methodology was motivated by an effort to test the blast resistance of structures subject to internal, or external, blasts where attention would be focused on areas such as joints, corners, or other areas within occluded geometry.

Three series of experiments were conducted in an effort to characterize the use of water bladders for blast simulations. Bladder material, geometry, use of baffles and strapping methods were varied along with Simulator input parameters such as impact velocity and impacting mass geometry. The effects of these variables have been quantified through the comparison of measured pressures, pulse durations and impulses. The experimental methodology demonstrates the ability to tailor load curves to simulate a wide range of blast scenarios.

© 2010 Published by Elsevier Ltd.

1. Introduction

A methodology has been developed to experimentally impose a wide variety of blast-like pressures and impulses to structures with complex geometry using non-explosive techniques. The technology was developed for the specific purpose of analyzing the structural resistance to blast loading of structures with complex, specifically joints, corners, or other occluded areas. Such needs have been detailed in many published reports, and including those concerned with complex geometries such as corners and joints (*e.g.* Lofti et al. 2009 [3], Kivity *et al.* 1993 [1], Sevin *et al.* 1995 [2], Walker *et al.* 1991 [4]). The cited references noted deal with a very wide range of structures including civil structures such as buildings, naval structures, off-shore structures, and a quite general range of "generic protective structures" as in [1]. The methods are applicable to a wide range of civil, marine, ship, and aerospace structures constructed from steel and alloys, FRP composites, reinforced concrete, and other materials. Using the University of California, San Diego (UCSD) Blast Simulator, experimental procedures have been established and are being extended to various types of structures, including those constructed from advanced FRP composite materials. The detailed methodology, involving the development of water bag media used to transfer momentum between energetic flyers and the target specimens, along with a novel use of dynamic load cells used to measure point-to-point forces *vs.* time history, is described by Huson and Asaro [5]. Herein we summarize key features of this methodology and its capability, the latter accomplished *vis-à-vis* the description of some specific results on structures with the configuration of joints or of regions either exterior or interior characterized by regions of high curvature. A key feature of the method, detailed below, is the use of various material media that may be shaped to fit complex geometries; the specific example of a material media described here is water. A key advantage of the Simulator methodology is the achievement of realistic blast-like pressure/impulse *vs.* time profiles without the use of explosives and associated fireballs and peripheral damage to instrumentation. Thus we are able to employ high speed photography, and a wide range of instrumentation including, *inter alia*, localized dynamic pressure transducers, strain gages, LVDT's, accelerometers, all of which are synchronized *via* timing software described herein to document critical deformations modes and the onset and mechanisms of structural damage.

The UCSD Blast Simulator, illustrated in Fig. 1, is a one-of-a-kind system, currently able to simulate explosive events without the use of explosive materials and therefore without the associated fireballs. This is accomplished with an array of high velocity hydraulic

---

* Corresponding author. Tel.: +1 858 534 6888; fax: +1 8584887818.
   E-mail address: rasaro@ucsd.edu (R.J. Asaro).

Target specimen   Flat flyers (aka programmers)

Reaction wall

Reaction wall
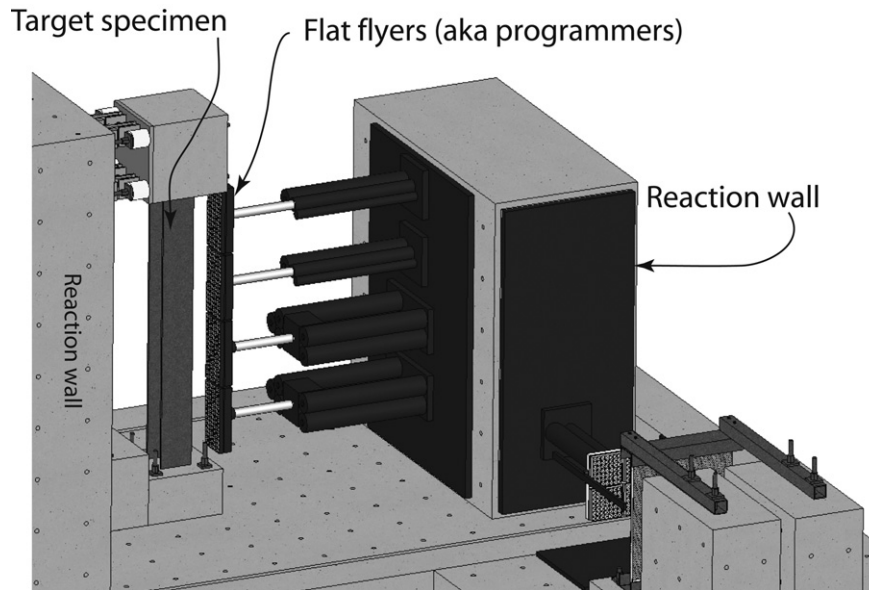
Fig. 1. Schematic representation of the UCSD Blast Simulator.

actuators driven by a combined high pressure nitrogen/hydraulic energy source. In explosive field testing, video and data from instrumentation is often lost to the destructive nature of the blast environment. The simulator allows for the generation of high fidelity data that documents the response and progression of failure associated with various realms of critical blast-like loading. Each actuator, referred to as a Blast Generator (BG), is depicted in Fig. 2, illustrating locations of impacting mass, control valves, transducers and accumulators.

To achieve the necessary pressures, nitrogen is first pumped into an accumulator where a volume of oil is compressed to high pressure (5000 psi). The oil flow into the acceleration port of the actuator is regulated through ultra high speed servo controlled poppet valves. The poppet valves are opened and the pressurized oil drives the piston/impacting mass assembly towards the specimen. At impact, a smaller servo controlled, return poppet valves opens, and a declaration chamber filled with pressurized nitrogen forces the oil out, retracting the impacting mass. Pressure transducers and magnetostrictive position sensors give precise feedback on the accumulator pressures and impactor positions. User supplied inputs such as impacting mass, velocity-time history, chamber pressures and valve timings all play critical roles in the control of the instrument. The UCSD Blast Simulator is described in detail, including calibration of the device, by Hegemier et al. [6].

Also described herein is the implementation of dynamic load cells, that may be prudently positioned within the target specimen,

that precisely record point-to-point data on induced force vs. time. This is vital for specimens of complex geometry and nonuniform shape. The dynamic load cells used are manufactured by Dytran Inc. They are piezoelectric force transducers which are available with capacities of 100 lbs–5000 lbs. They are no more than 0.75″ in diameter and are 1.25″ long. They are directly connected to our DAQ systems and provide immediate (i.e. with a resolution of less than 0.1 ms) response to the impulsive loading seen in the blast simulations. The additional use of strain gages, LVTD's etc. is, of course, also routinely employed as described via the examples reviewed below.

Further calibration of the Simulator on flat geometries has been demonstrated through a wide range of structural applications. The ability to simulate blast loading was first demonstrated on concrete columns and is described in detail in Rodriguez [14]. This research included details on the construction of the Simulator, comparison to field tests, and the development of hardening techniques for rectangular columns. Application to masonry walls is documented in Oesterle [15]. These experiments investigated the structural behavior of polyurea reinforced masonry and FRP retrofitted reinforced concrete walls when subjected to simulated blast loads. The use of the Simulator to impulsively load steel W-sections and comparisons to explosive testing are described in Stewart et al. [16].

In order to distribute blast-like loads on non-flat geometries, confined water was combined with specifically shaped impacting masses. As demonstrated below, the technique enables the

Programmer
Reaction Mass   Accelerometers   8.0 Gal Accumulator
                                       N2 2000 psi (variable)   Pilot Pressure
          N2 Fill Port   LVDT
                        Pressure Transducers   ◁ 1000 psi

                                                                                    ◁ 50 psi
                                       2.75 Gal Accumulator   Pilot Return
                                       N2 50 psi (variable)   Return

          Piston Rod   Deceleration Chamber   Acceleration   Poppet Valves
                          N2 500 psi (variable)   Chamber, Oil
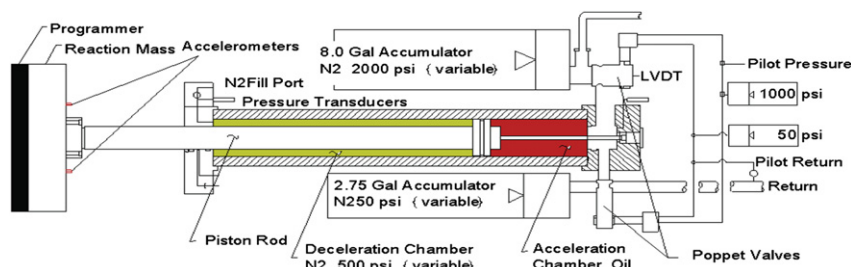
Fig. 2. Schematic of a Blast Generator (BG).
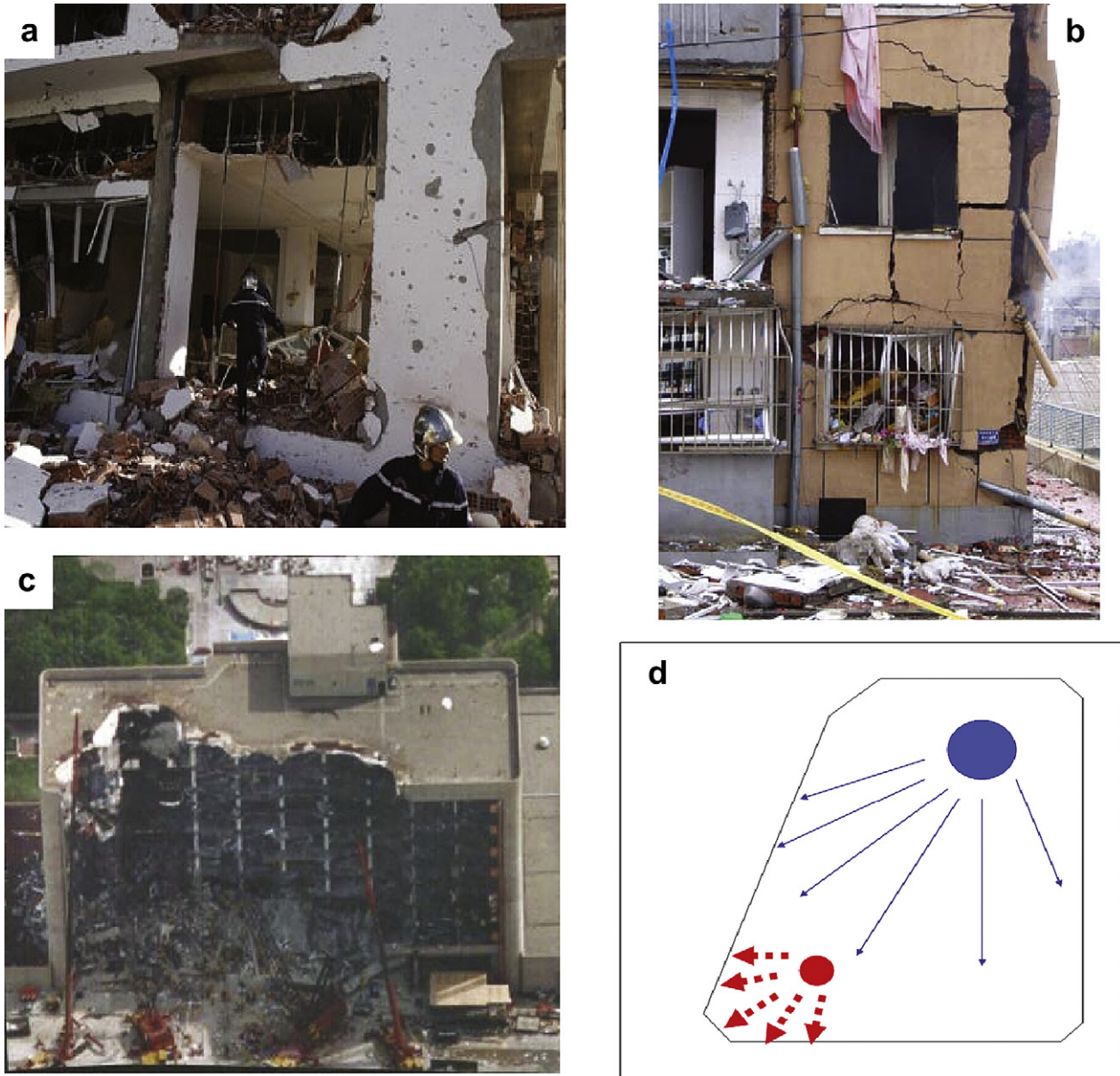
Fig. 3. Blast effects on civil structures. (a) Internal blast of unknown origin and type in a 12 story building at the Russian Black Sea Resort in Sochi, Russia, (b) Internal blast caused by a gas leak within an apartment building in Dalian in China's northeast Liaonong Province, (c) external blast (truck bomb) at the Alfred P. Murrah Federal Building in Oklahoma City 1995, (d) Schematic showing two blast scenarios. Smaller charge located close in to a corner region (red) and larger charge located further out and possibly asymmetrically with respect to the corner's center.
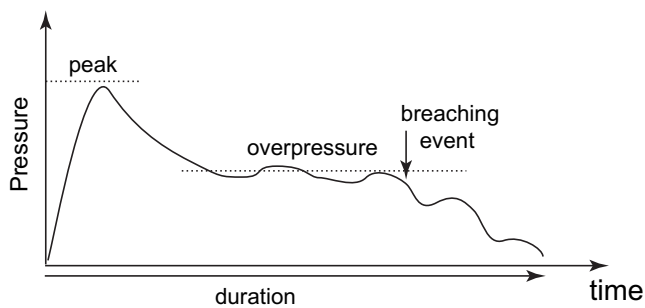
Fig. 4. Schematic representation of the pressure *vs.* time history following a blast. Peak pressures are followed by a decay to a continuing overpressure regime which is terminated by a breaching event caused by a structural failures allowing gases to escape.

tailoring of pressure *vs.* time histories so as to simulate a wide range of multi-dimensional blast scenarios onto various structures of interest. In what follows below, it is demonstrated that the Simulator techniques produce realistic blast-like pressure/impulse vs. time histories on both flat panel structures as well as those characterized by regions of high curvature. An example of a comparison between blast field data and Simulator results as well as

Table 1
Material properties for the two selected material systems.

Material type	Fabric type	Thickness (in)	Weight (oz/yd^2)	Burst strength (lbf)	Tear strength (lbf)
XR5	Polyester	0.03	6.5	650	35
U1940	Nylon	0.045	13	1200	40

Fig. 5. Photo of typical vertical internal baffles used to control water flow within the bladders and provide additional structural reinforcement.

comparisons between Simulator data and CTH hydrocode simulations are provided in Sections 3.3 and 4, respectively.

The paper is presented as follows. In the next section we provide a brief overview of previously published studies of blast resistance of various structures. The purpose in this is to provide perspective on typical pressure-impulse vs. time environments of general interest. In the following section we describe the development and evaluation of a system of tailored bladders, *i.e.* water bags used to transfer momentum from our flyers to test specimens. Following this we describe the specific use of the water bag media in simulations of blast loading of structural sections of composite joint specimens. Our examples deal specifically with the nonuniform nature of pressure-impulse distribution as just noted. Discussion and conclusions then follow.

2. Blast pressure *vs.* time

As noted above, the interest lies in simulating blast-like loads imparted onto structures with complex geometry, for example civil structures such as buildings (see Fig. 3 for specific examples). The examples shown illustrate blasts that were either exterior or interior to the structures, but in all cases the structures contained complex geometries such as corners, joints, overhangs, doors, rooms, *etc*. The distribution of stresses and deflections induced by the loading and the resulting progression of damage and eventual breaching and failure, were strongly mediated by the geometry as well as by the characteristics of the loading itself. As illustrated in Fig. 3d, the pressures associated with the blast are distributed within the regions of interest and, in fact, the actual distributions of imposed pressure (and impulse) are spatially and temporally nonuniform. The cases schematically illustrated are intended to show that depending on location with respect to a region such as a corner, loading may vary as a function of distance and position of the charge. Examples are presented below that further illustrate the variability in possible threat scenarios.

Details about blast loading in the open literature have focused on the description of overpressure pulse measurements onto full-scale walls and onto smaller-scale test panels. A selection of these are summarized for the purpose of describing the range of pressures and duration of pulse that are relevant to the topic of blast loading onto structures. Also described is our approach to assess blast induced pressures *vs.* time histories *via* hydrodynamic simulation.

Jacinto *et al.* [7] conducted a series of air-blast tests to measure overpressure pulses and dynamic response of plates for explosive charges ranging in mass from 2 lb to 20 lb (0.8–10 kg) set at various distances from 100 to 200 ft (30–60 m) from target plates of 3–6.5 ft² (1–1.5 m²) in area. They measured pressure pulses with a generic shape as sketched in Fig. 4; such pulses had an almost
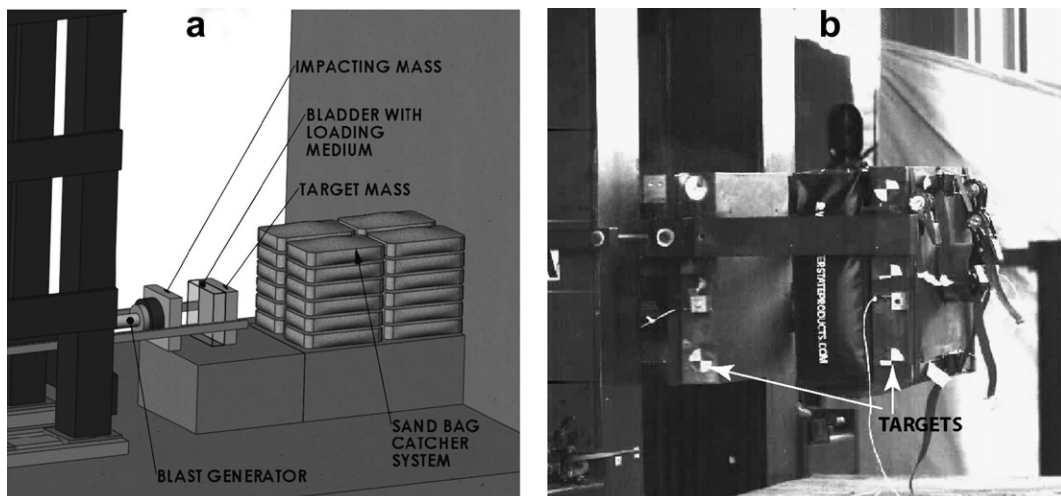
Fig. 6. (a) Schematic and (b) photo of 1-D Plate Impact Tests.
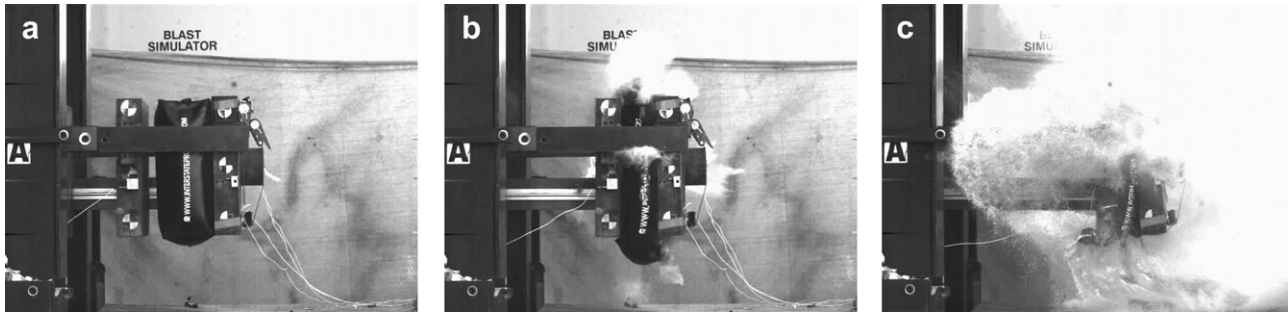
Fig. 7. Sequence of events during a 1-D impact. (a) Before impact, (b) at impact, (c) after impact.

immediate rise to peak pressures in the 0.15 to 1.5 psi(1–10 kPa) range with pressures tapering-off over durations of up to 10 ms. Scherbatiuk and Rattanawangcharoen [8] conducted open air-blast tests on free-standing soil-filled Concertainer walls and measured pulses of similar shape and of magnitudes in the range 115–870 psi (0.8–6 MPa) and lasting for durations of 3–8 ms. Concertainer are folded wire mesh geotextile lined cubical connected baskets; pressure gauges were positioned on the outer concertainer walls. Thus after peak pressures were attained, the pressures expectedly dropped off in the above mentioned time periods. In still other experiments, peak and overpressures pressures were measured by Houlston *et al.* [9] in the range 10 psi to nearly 600 psi (50 kPa–4 MPa) for durations of 1–2 ms in for blasts onto test plates. Details of charge type and mass were not provided, but it is notable that at the higher pressures attained the durations were reduced to no longer than 1 ms. Davidson *et al.* [10] measured peak pressures in the 45 psi (300 kPa) range with durations of roughly 10 ms for blasts onto polymer-reinforced concrete masonry walls. There are reports of blast induced pressures as directly related to ship structures as the following examples illustrate.

Slater [11] investigated blast resistance of glass fiber reinforce plastic (GRP) composite panels for use in Naval ship structures. Up to full-scale test panels, with dimensions 9 ft × 16 ft, were subject to explosive blast loading. Measured pressure pulses reported were of the generic shape illustrated by Fig. 4, with peak pressures of 15–60 psi (105–405 kPa) (classified as moderate and severe conditions, respectively) and durations of 50–100 ms for panel and beam specimens, and 200 ms for the full-scale test panel. We note that these tests were reported to simulate threats associated with nuclear blasts.

Methods for investigating blast damage to composites by smaller-scale test specimens were reported on by Mouritz [12] who studied underwater blast loading onto relatively small (10 in × 3 in) stitched composite test specimens by suspending 1–1.75 oz (30 or 50 g) of explosive 3 ft (1 m) distance away from the specimen under water. These produced low and high intensity blast overpressures, with peak pressures reaching 1885 psi and 3625 psi (13 and 25 MPa), respectively, as measured by a pressure sensor mounted onto the specimen surface. The pulses were roughly triangular in profile, with an almost equal rise and decay time, lasting 20–35 μs and were used to excite damage, *via* delamination cracking, in the test specimens.

Additional detail concerning typical peak and overpressures accompanying a wide array of blast environments can be found in standard sources such as Bulson (1997) [13].

Surveys such as these, therefore, show that blast peak pressures of typical interest lie in a rather broad range of say, 75–1450 psi (500–1000 kPa), with overpressure durations ranging from 0.5 to 10 ms or even higher. Of course, we note that in practice, and most particularly for blasts occurring within closed compartments, overpressure durations are controlled by the onset and development of breaching events caused by structural failure. Thus our interest here will be limited to durations of ≤10 ms.

3. Water bag media: water confinement method

The first requirement for using fluid media was to find an appropriate and controllable confinement method. Woven polyester and nylon fabrics *geomembrane* material system produced by Seamen Inc. were adopted based on the material's tear strength and burst resistivity. Such bladders are typically used for large scale water containment purposes as well as hazardous material control. Two material systems were selected for testing, an XR-5 polyester system and U1940 Nylon system. Material properties for the bladders are presented in Table 1.

The bladders were manufactured to design specifications by Interstate Products Inc. The design incorporated baffling for shape reinforcement, strapping eyelets used to mount the bladders on
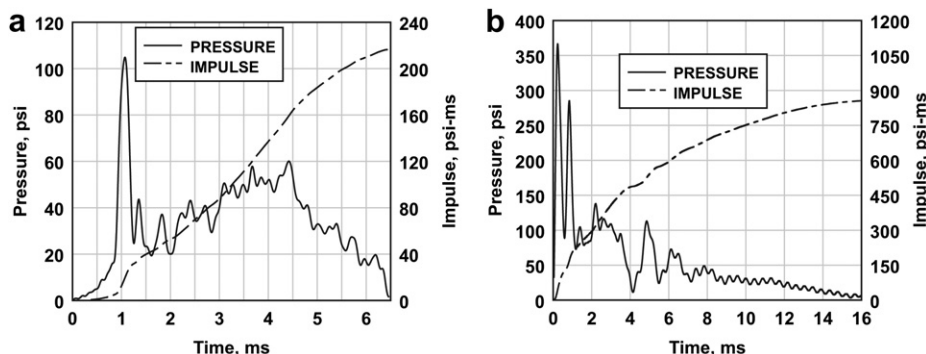
Fig. 8. Typical pressure-impulse *vs.* time profiles for 1-D plate impact tests 1a and 2b.

Table 2
Summary of key parameters and results from six impact tests.

Test	Bladder type	Depth (in)	Velocity (m/s)	Baffles	Peak pressure (psi)	Duration (ms)	Impulse (psi-ms)
1	XR5	6	15	No	120	6	240
2	XR5	6	15	Yes	370	16	875
3	XR5	6	10	No	80	6	170
4	U1940	6	15	No	180	7	500
5	XR5	8	20	No	200	27	2350
6	XR5	6	25	Yes	145	3	90

specimens and variation in both material thickness and valve design. One of the primary aims of these experiments was to examine the tailorability of resultant pressure time histories by varying bag geometry and Simulator input parameters. Through the variation of velocity and impact mass, peak pressures were able to be controlled. Changing bladder material, thickness, width, baffling, and valves type allow for the modification of pulse duration, while bladder and impacting mass geometries governed the spatial distribution of applied pressures over time. Of particular importance to the design of effective water bladders is the design of their internal baffling as shown, as an example, in Fig. 5. The purposes of the baffles are, *inter alia*, to control the flow of water within the bladders, and to provide additional structural reinforcement. These effects, in turn, aide in regulating the bursting of the bladders and the shape and duration of the induced pressures pulses. The effects of these variables are discussed in the subsequent sections.

As noted in the previous section, a typical range of blast pressure to be imposed on a wide range of civil, off-shore, naval, marine, and aerospace structures lies in the range of 75–1500 psi(0.5–10 MPa). Accordingly, we chose to focus most of our initial studies within this range. We note, however, that other ranges are often of interest and thus to demonstrate even further capability, we have included examples where peak pressures of $\geq$42 MPa (or 6000 psi) are achieved as well as durations exceeding 20 ms. Most noteworthy is that these high ranges of pressures are achieved within the same experimental configuration as is used for the much lower range, thereby demonstrating the versatility of our methods.

3.1. 1-Dimensional tests and water bag evaluation

The initial experiments conducted concerned the effects of bladder material selection and geometry. The 16″ × 16″ bladders

were mounted on a 16″ × 16″ × 3″ steel plate and then placed in front of the impacting mass. Piezoelectric force transducers were embedded in the steel plate. A 16″ × 16″ × 3″ steel flyer plate was used to impact the bladder/plate target and pressures produced were measured with the transducers. Ultra high speed Phantom cameras (Vision technologies, Inc) were used in conjunction with *TEMA* tracking software to record experiments at 5000 to 10,000 frames per second. Targets placed on both impacting and target specimens allowed for tracking of displacement, from which velocity and acceleration can also be computed. A schematic of the setup is shown in Fig. 6. The experimental sequence of events is shown in Fig. 7. Desired velocities of the impacting mass are governed by designation of oil and nitrogen pressures along with timed valve controls. The impacting mass is accelerated towards the bladder/steel target and makes initial contact with the bladder. The resulting shock wave propagates through the water towards the boundaries of the bladder and initiates breach. This is illustrated in Fig. 8: a fast rise in pressure followed by a sharp drop is seen as the bladder breaks. The subsequent overpressure continues until all the water has been dispersed. A summary of the 1D Plate Impact tests that lists results for some key parameters of the tests is provided in Table 2.

Table 2 summarizes the input parameters and results for the first round of plate impact tests. The role of baffling can be seen in the differences between Tests 1 and 2. The baffled bag provided a 10 ms increase in the duration of the pulse and over three times the peak pressure. The use of baffles also improved the shape of the bladder, creating a more uniform flat surface of impact. The effect of material selection can be seen between tests 1 and 4. The thicker nylon U1940 bladder created a peak pressure of 180 psi and duration of 7 ms compared to the 120 psi peak pressure and 6 ms duration of the polyester XR5 bladder. The large difference in the impulse, 240 psi-ms compared to 500 psi-ms, is due to the reflections created by the strength of the U1940 material. The wave was reflected within the bladder and reached the peak pressure three times before bursting, creating the larger impulse. Examining tests 1 and 5, a significant effect can be seen in the variation of bladder depth. The difference in peak pressure can be attributed to the higher impact velocity The 8″ bladder produced a duration of 27 ms, leading to an impulse of 2350 psi-ms. The larger bladder increased target mass, which in turn decreased the velocity of the flyer plate and increased the duration of the pulse. Changes in impact velocity also had significant effects. A decrease of 40% in impulse is observed by decreasing the velocity from 15 m/s to 10 m/s in tests 1 and 3.
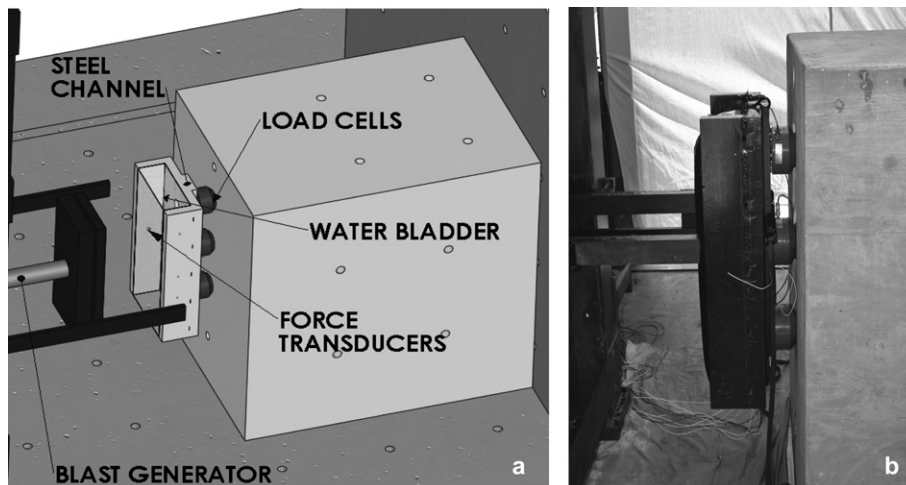
Fig. 9. (a) Schematic and (b) photo of channel tests set up.
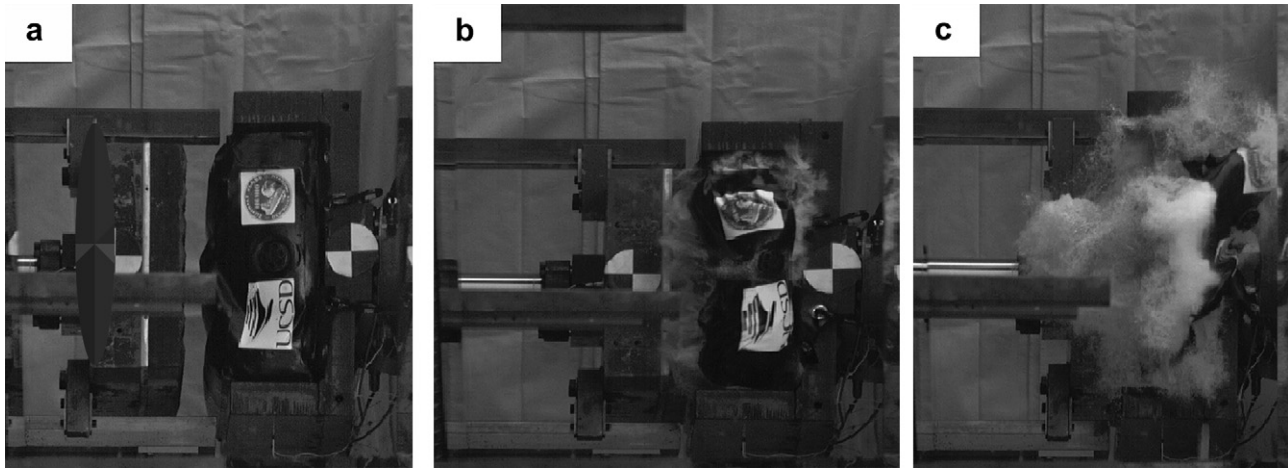
Fig. 10. Sequence of events of 2D impacts. (a) Before impact, (b) at impact, (c) after impact.

However, increasing the velocity to 25 m/s and adding baffles created a different result. Due to a lack of exterior confinement, the bladder breached almost instantaneously, decreasing the mass of water reaching the plate as well as the duration, resulting in an impulse of only 90 psi-ms. This last result will be scrutinized closely in the following section where the impact is confined in two additional directions.

3.2. 2-Dimensional geometrical confinement: channel tests

The second round of tests were conducted in an effort to document "2D" pressure resultants. For an actual blast in enclosed geometries, pressures are generated as a function of geometric confinement and interactions of primary and reflected waves. In many cases this process will result in a sequence of pressure peaks in multiple directions. To test the simplest of cases, a blast wave into a 90° geometry was simulated. A 2″ deep steel channel was designed to measure both normal and lateral pressures, without deforming the specimen. The channel and channel setup are shown in Fig. 9.

Force transducers were mounted in different locations along all three faces of the channel, and three 50 kip load cells were mounted to measure total force imparted onto the specimen. Input parameters of interest included actuator velocity, depth of bladder, and bladder material. The channel was mounted on a custom concrete block which acted as an anchor for the test and allowed for the actuator to be retracted instead of launched. Mirrors were

mounted to produce overhead camera views of the experiment and assist in measurements. The sequence of events *via* the overhead mounted mirror is shown in Fig. 10.

Table 3 summarizes the input parameters and results of the 2D Channel Tests and Fig. 11 denotes typical results. All bladders were baffled and pressure measurements were made on both the normal and lateral faces of the channel. The values presented in Table 3 are averages over multiple pressure transducers positioned along each side.

The effects of velocity can be clearly seen *via* the comparisons of tests 1, 2, 5 and 9. As the velocity was increased, both normal and lateral pressures were increased. An increase from 276 to 394 in/s (7–10 m/s) produced a 17% in normal impulse with a 3% increase in lateral impulse. An increase from 394 in/s (10 m/s) to 512 in/s (13 m/s), produced a 50% increase in normal impulse, with only a 16% increase in lateral pressure. Increasing the velocity from 512 in/s (13 m/s) to 1181 in/s (30 m/s) produced impulses on the order of 40% for normal pressures, but created almost double the lateral impulse. The same comparison can be made between tests 6 and 8 for the 4″ deep bladder. An increase of 394 in/s (10 m/s) increased both normal and lateral impulses by 40%.

The result of varying bladder depth for the 2D cases can be seen between Tests 1 and 3 and Tests 6 and 7. The smaller bladder produced greater pressures and impulses at a velocity of 10 m/s, where as the larger bladder produced the larger pressures and impulses at a velocity of 30 m/s. This suggests that bladder geometry has a greater effect at lower velocities, whereas at higher velocities bladder geometry becomes less significant.

Material property comparisons can be made through analysis of tests 5 and 6 and tests 8 and 9. At an impact velocity of 20 m/s, the U1940 nylon bladder exhibits a 40% increase in both normal and lateral pressures over the XR5 material. However, at 30 m/s the XR5 shows slightly larger impulses in both the normal and lateral directions. This is consistent with the conclusion that at higher velocities, small variations in bladder type and geometry have less of an effect than at lower velocities. It is worth noting that impacting the XR5 material at a velocity of 30 m/s produced almost identical results to the impact of a U1940 bladder at 20 m/s.

3.3. Comparison of simulator with field blast testing

Simulator tests as just described have been directly compared to actual blast test results conducted in field tests as illustrated in Fig. 12. The similarities in results can be seen in the pressure time

Table 3
Summary of 2D channel tests.

Test #	Bladder Type	Depth (in)	Velocity (in/s) (m/s)	Peak Normal pressure (psi)	Peak Lateral pressure (psi)	Normal impulse (psi-ms)	Lateral impulse (psi-ms)
1	XR5	6	276 (7)	600	630	1460	1780
2	XR5	6	394 (10)	610	620	1720	1840
3	XR5	4	394 (10)	1050	1120	1640	1660
4	XR5	4	512 (13)	1328	1054	1750	1750
5	XR5	6	512 (13)	880	790	2675	2135
6	XR5	4	787 (20)	2000	2150	1750	1775
7	U1940	4	787 (20)	2840	3000	2270	2525
8	XR5	4	1181 (30)	2840	3000	2285	2520
9	XR5	6	1181 (30)	3475	3800	3875	4240
10	U1940	6	1181 (30)	4000	6200	3690	3690
11	XR5	4	1181 (33)	4312	3692	6696	4651
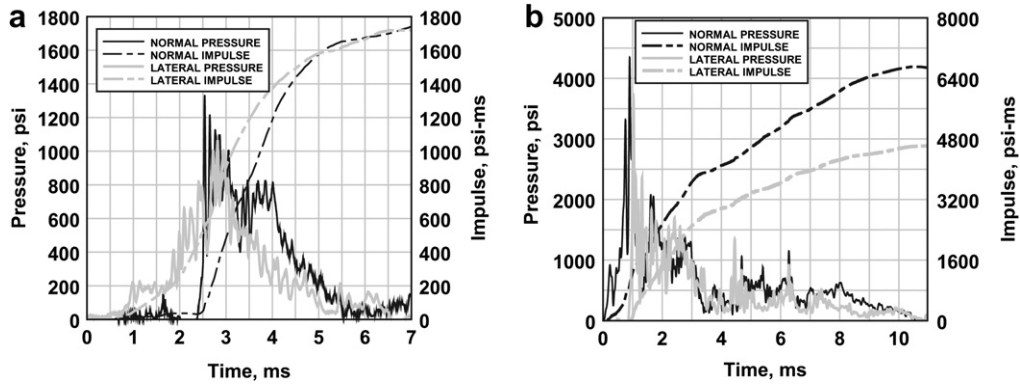
Fig. 11. Typical pressure-impulse *vs.* time responses within the channel, Tests 4 (a) and 10 (b).

history comparison of simulator tests (a) and actual field tests (b). Although different in magnitude, the characteristics to an actual blast pulse are clearly demonstrated: a peak incident pressure, followed by a decay to ambient pressure in a duration of milliseconds. Depending on the threat scenario, the method can be engineered to create the associated pressure time history in magnitude, duration and shape. In terms of structural response, the impulse, or area under the pressure time curve, can be of most interest, allowing flexibility in the tuning of Simulator and/or water bladder parameters and still procuring structural behavior of interest.

4. Simulated blast loading of joints: trapezoidal *vs.* round flyers

4.1. Uniformly distributed pressure/impulse vs. time history

Of primary importance in the present study is the ability to impart blast like loads onto corner-like regions associated with enclosed regions such as rooms, compartments, or even exterior regions characterized by having corners facing a blast wave. Prototype composite sandwich joints were constructed either from plywood with foam cores or FRP composites with wood cores for preliminary testing in the form of acute, 90° and obtuse angles. A third set of experiments focused on impacting mass/bladder geometry and its role in the spatial and temporal distribution.

The numerical hydrocode, CTH, was used to gain insight on the effects of charge size and location on pressure wave arrival. 2D geometries of typical joint sections were employed in all CTH calculations. Tracers were placed in points of interest, allowing for the measurement of pressure throughout the duration of the simulations. Reflective, rigid boundary conditions were used in all directions, and the compartment was filled with air at atmospheric pressure using Sandia National Laboratory's SESAME model for non-explosive materials. A charge of Composition C4 was modeled using a JWL equation of state to simulate the adiabatic expansion of the detonation products [17]. A scaled distance (the ratio of distance over the cube root of the charge's weight) of $Z = 0.75$ was used in all simulations.

For charges closer to boundaries, a CTH calculation presented in Fig. 13a, demonstrate the virtual simultaneous arrival of pressure to the middle and side of a typical joint section. To simulate this blast environment, a 0.5″ trapezoidal steel flyer was designed along with a complimentary shaped trapezoidal bladder. Force transducers were inserted into the specimen at various locations along the joint, seen in Fig. 14a. The pressure time histories can be see in Fig. 14b. The desired effect is demonstrated by the arrival of the pulses, all within 1 ms of each other.

4.2. Non-uniformly distributed pressure vs. time

For charges located towards the center of closed regions, a CTH calculation presented in Fig. 16 demonstrate the progression of a blast wave arrival first along the boundaries and subsequently towards the joints (*i.e.* corners). That is, the walls of the enclosed region are loaded first, and the wave then subsequently propagates along the wall towards the joint.

To simulate this threat scenario, a 0.5″ thick, semi-hemispherical steel flyer was designed along with a shaped trapezoidal bladder. The bladder was designed to be 4″ thicker in the middle to
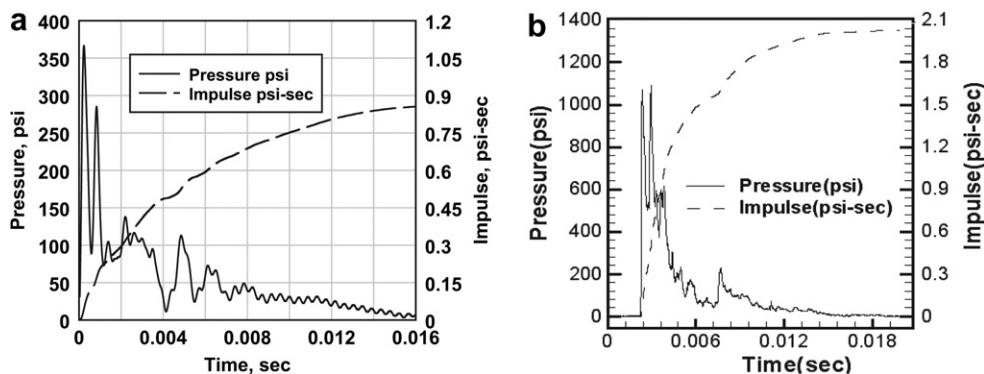
Fig. 12. (a) Simulator test using a bladder. (b) Field test results from a blast set against a civil column structure.
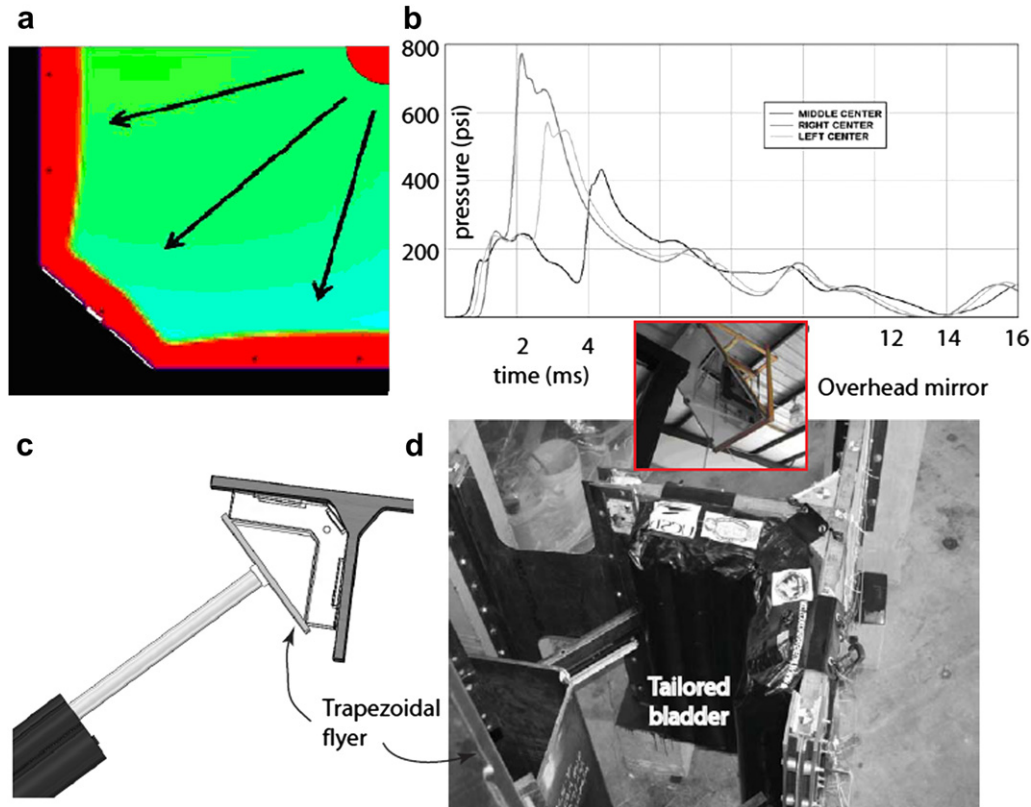
Fig. 13. Test design for charges near boundaries: (a) CTH simulation set up, (b) computed pressures *vs.* time at various tracer locations, (c) schematic of experimental set up, (d) photo of experimental set up.

simulate the arrival of both primary and reflected waves seen in CTH calculations. Force transducers were inserted into the specimen at various locations along the joint, seen in Fig. 16a. The pressure time and impulses time histories can be see in Fig. 17b. The desired effect is demonstrated by the arrival of the pulse sequentially, beginning towards the arms of the joint, and propagating towards the middle face of the joint.

5. Discussion

Among the many questions that arise in assessing the phenomenology of damage incurred during blast-like loading is the effect of details such as the undulations, or fluctuations observed in the pressure *vs.* time profiles evident, for example, in Figs. 8, 11,14 and 16. Combined with analysis *via* FEM simulation, the Blast
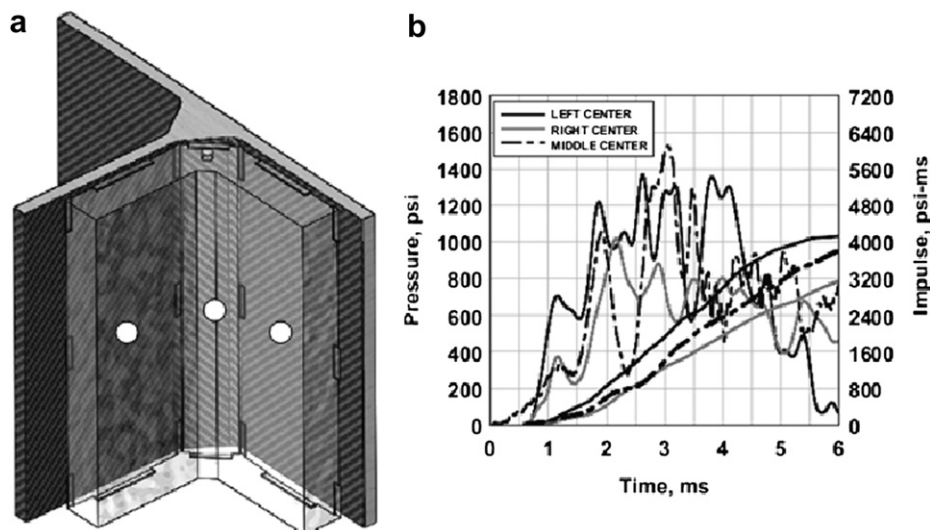
Fig. 14. Test design for charges near boundaries: (a) schematic of experimental set up, (b) experimentally measured pressures *vs.* time at various locations of dynamic load cells.
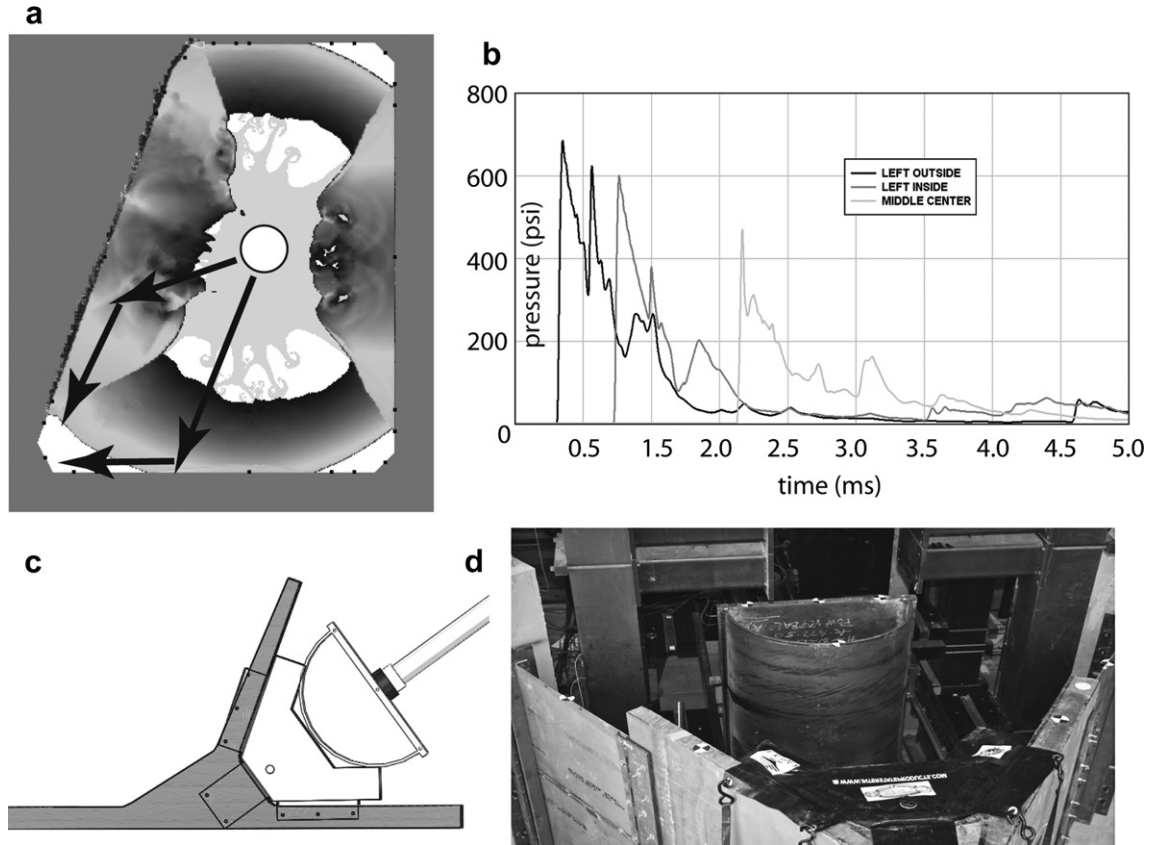
Fig. 15. Test design for charges further from boundaries: (a) CTH simulation set up, (b) computed pressures *vs.* time at tracer locations, (c) design, (d) experimental set up using semicircular flyer and trapezoidal bladder.

Simulator methods may be used to quantitatively assess the importance of such detail.

As an example, the experimentally generated blast-like pressure *vs.* time profile shown in Fig. 17b was imposed upon a composite joint structure within a LS-DYNA simulation [18]. The explicit finite element model was conducted under plain strain conditions and composed of approximately 40,000 elements. The CFRP/Balsa/CRFP sandwich structure was reacted using steel gripping fixtures mounted to pre-tensioned concrete blocks. Geometry and dimensions of the test setup simulation can be seen in Fig. 17a. Typical 9.5 lb/ft^3 Baltek SB Structural End-Grain Balsa material properties ($Ex = 581.2$ ksi, $Ey = 22.0$ ksi, $Gxy = 23.2$ ksi) were assigned to the core, and effective laminate properties ($Ex = Ey = 6.1$ msi, $Gxy = 2.2$ msi) were used for the CFRP facesheets.

A snap shot at 0.75 ms of the resulting contours of maximum shear strain in the balsa core is shown in Fig. 17c; the maximum value of the maximum shear strain *vs.* time is shown in Fig. 17d. In contrast, a "smoothed" pressure *vs.* time profile was constructed so as to produce a similar impulse *vs.* time profile, as is also shown in Fig. 17b. A parallel FEM simulation was performed using this idealized yet impulse similar profile. Our focus was placed on the maximum core shear since experiments as described in Figs. 13 and 15 have consistently shown that failure of such joint structures is initiated by core shear failure values approaching 1% shear strain.
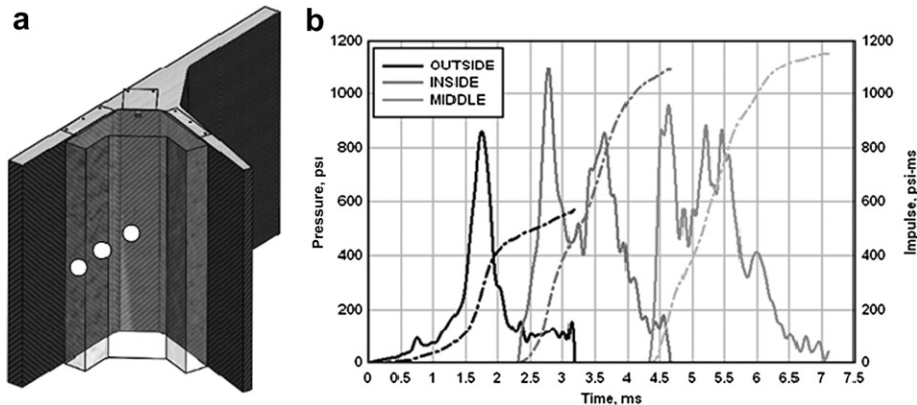
Fig. 16. Test design for charges near boundaries: (a) Schematic of experimental set up set up, (b) experimental pressures *vs.* time at locations of dynamic load cells.
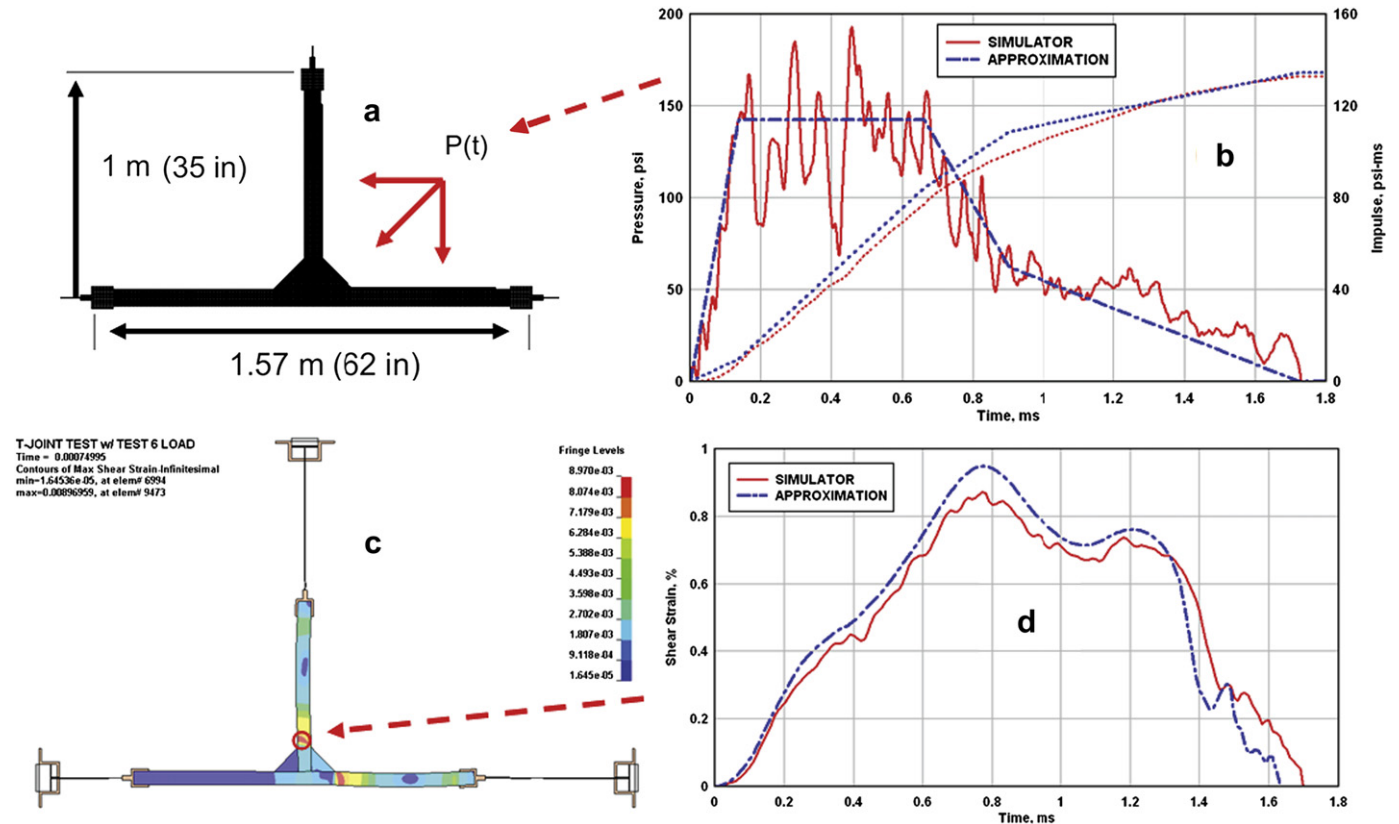
Fig. 17. (a) Specimen geometry and loading conditions (b) measured pressure *vs.* time profile illustrating undulations, or fluctuations, in measured pressure *vs.* time and approximation that yields a similar impulse *vs.* time profile. (c) Contours of maximum shear strain (d) Shear strain history in balsa.

The results for the maximum shear strain in the core are shown for both simulations in Fig. 11d and as may be readily noted, the results are quite similar. In fact, we noted that the results for the overall deflections of the joint specimens as well as the stress and strain states were quite similar in both simulations. Thus we conclude from this that failure of the joint would occur in a similar manner under both scenarios. As such details within the pressure *vs.* time profiles are indeed quite variable, dependent on the details of the blast, *e.g.* charge size, location, symmetry *vis-à-vis* the joint's center, such insight becomes invaluable in assessing the general effects of typical blasts of joint survival.

6. Summary and conclusions

UCSD has developed a technique to simulate blast loading in structures of complex geometries. The method combines the UCSD Blast Simulator and custom water bladders to produce multi-directional impulsive loads. Three series of tests were conducted in an effort to characterize the experimental technique: 1D Plate Tests, 2D Channel Tests and a set of Joint Tests.

It has been demonstrated that the pressure-time histories and resulting impulses can be tailored to specific threat scenarios. Through the variation of bladder geometry, material selection, baffling, actuator velocity, and impact mass geometry, spatial and temporal distribution of the impulsive loads were quantified and compared.

The motivation of these experiments was to develop a method in which to determine the structural blast resistance of a wide variety structures. The data so obtained may be used to calibrate input parameters and assist in quantifying loads imparted onto structures or sections of structures of interest. Validated numerical simulations of the water bladders themselves will also assist in

selection of appropriate bladder characteristics for future Simulator experiments.

References

[1] Kivity Y, Florie C, Lenselivk H, 1993. Response of Protective Structures to Internal Explosions with Blast Venting, MSC World Users Conference.
[2] Seven E, Knoop SL, Belytschko T, Briggs GG, Hall WJ, Hoffman B, et al. Protecting buildings from bomb damage. Washington DC: National Academy Press; 1995.
[3] Lofti H, Tarfaoui M, Vautin A. Design and test of a sandwich T-Joint for naval ships, in damage, Fracture Mechanics, and failure analysis of engineering materials and structures. Netherlands: Springer; 2009.
[4] Walker S, Chunsheng H, Williams JR, Offhore W, 1991. Assessment of the blast resistance of off-shore topside structures, Offshore Technology Conference, May 1991.
[5] Huson P, Asaro RJ, 2009. Non-Explosive Methods for Simulating Blast Loading of Structures with Complex Geometries, Blast on Structures with Occluded Geometry: UCSD Project "Methods for Simulating Blast Loading of Structures with Complex Geometries": Report #1.
[6] Hegemier GA, Stewart L, Seible F, 2007. The UCSD Blast Simulator. In: 77th Shock and Vibration Symposium, Montery, CA, March.
[7] Jacinto AC, Ambrosini RD, Danesi RF. Experimental and computational analysis of plates under air blast loading. International Journal of Impact Engineering 2001;25:927–47.
[8] Scherbatiuk K, Rattanawangcharoen N. Experimental testing and numerical modeling of soil-filled concertainer walls. Engineering Structures 2008;30:3545–54.
[9] Houlston R, Slater JE, Pegg N, DesRochers CG. On analysis of structural response of ship panels subjected to air blast loading. Computers and Structures 1985;21:273–89.

[10] Davidson JS, Fisher JW, Hammons MI, Porter JR, Dinan RJ. Failure mechanisms of polymer-reinforced concrete masonry walls subjected to blast. Journal of Structural Engineering 2005;131:1194–205.

[11] Slater JE. Selection of a blast-resistant GRP compsite panel design for naval ship structures. Marine Structures 1994;7:417–40.

[12] Mouritz AP. Ballistic impact and explosive blast resistance of stitched composites. Composites: Part B 2001;32:431–9.

[13] Bulson PS. Explosive loading of engineering structures. New York, NY: E & FN Spon; 1997.

[14] Rodriguez T, 2008. The UCSD Blast Simulator: Experimental Methodology, Ph.D Dissertation, University of California, San Diego, La Jolla, California.

[15] Oesterle M, 2009. Blast Simulator Wall Tests: Experimental Methods and Mitigation Strategies for Reinforced Concrete and Concrete Masonry, Ph.D Dissertation, University of California, San Diego, La Jolla, California.

[16] Stewart L, Hegemier G, Morrill K, 2009. Simulated Blast Testing of Structural Steel Columns. In: 8th International Conference on Shock and Impact Loads on Structures, Adelaide, Australia.

[17] Bell RL, Baer MR, Brannon RM, Crawford DA, Elrick MG, Hertel Jr ES, et al. CTH user's manual and input instructions version 7.1. Albuquerque, NM: Sandia Nat Lab; January 2006.

[18] LS-DYNA. LS-DYNA Keyword User's Manual, Version 971, vols. I and II. Livermore CA: Livermore Software Technology Corp; 2007.